Effects of Phenanthroline Type Ligands on the Dynamic Processes of (η^3-Allyl)palladium Complexes. Molecular Structure of (2,9-Dimethyl-1,10-phenanthroline)[(1,2,3-η)-3-methyl-2-butenyl]-chloropalladium

Sverker Hansson, Per-Ola Norrby, Magnus P. T. Sjögren, and Björn Åkermark*

Department of Organic Chemistry, Royal Institute of Technology, S-100 44 Stockholm, Sweden

Maria Elena Cucciolito, Federico Giordano, and Aldo Vitagliano*

Dipartimento di Chimica, Università di Napoli "Federico II", Via Mezzocannone 4, I-80134 Napoli, Italy

Received June 16, 1993®

Using saturation-transfer experiments and measurements of coalescence temperatures, the effects of phenanthroline ligands on the activation parameters for syn–anti isomerization, syn–anti proton exchange, and apparent rotation in six (η^3-allyl)palladium complexes have been studied. The rates of the processes are increased by the addition of ionic, coordinating ligands such as chloride indicating a pentacoordinated intermediate. By X-ray crystallography the structure of a potential intermediate of this type has been determined. Finally, using 2-(8-methoxy-1-naphthyl)-1,10-phenanthroline, it has been possible both to observe chiral induction on a deuterium-substituted η^3-allyl group and to find additional information on the mechanism of apparent rotation.

Introduction

Palladium-catalyzed nucleophilic displacement of allylic acetate is an important example of a metal-catalyzed process where the formation and reaction of η^3-allyl complexes are essential steps.[1] We have shown recently that the use of 2,9-disubstituted 1,10-phenanthroline ligands permits control of *Z* and *E* stereochemistry in the alkene product by regulating the anti and syn stereochemistry of the intermediate η^3-allyl complexes.[2] The effect of the substituents in the 2- and 9-position of 1,10-phenanthroline was shown to favor the anti isomer by a selective steric destabilization of the syn isomer.[2] In our continuing studies of the effects of 2,9-substituents, we also have found indications that chiral control may be possible.

The scope of ligand-induced control in nucleophilic additions depends on the relative rates of addition and the dynamic processes which are characteristic for (η^3-allyl)palladium complexes. In a classic review by Vrieze,[3] the experimental evidence for the most important dynamic processes has been summarized. The studies reviewed dealt mainly with second-row elements and heavier ligands (e.g. phosphines and chloride) where the dynamics commonly can be studied through coalescence phenomena. Already at that time, it was clear that the syn–anti isomerization takes place via an η^3–η^1–η^3 rearrangement.[4] For the syn–syn, anti–anti exchange (apparent rotation of the allyl group), several mechanisms have been suggested, but in at least one case, it was shown to be the result of fast ligand exchange.[5] In recent years, some studies have been performed on bidentate nitrogen ligands similar to 1,10-phenanthroline. However, the results from these studies are inconclusive. Crociani et al.[6] observed that chloride accelerated the apparent rotation without exchange of the bidentate ligand, indicating that the mechanism for exchange is pseudorotation in a pentacoordinate palladium intermediate as postulated previously.[3] An alternative mechanism, involving bond breaking to one nitrogen, rearrangement, and recombination, was postulated by Pregosin et al.[7] Because the relative rates of the dynamic processes and of the nucleophilic attack on the η^3-allyl system are crucial to regio-, stereo-, and enantiocontrol in catalytic reactions, we undertook an investigation of the active processes in complexes with substituted 1,10-phenanthroline ligands. Our aim was to elucidate the role of steric effects of 2,9-substituents on η^3–η^1–η^3 rearrangements as well as the apparent rotation of the allyl group.

Results and Discussion

In the early studies of the crotyl complexes **1** and **2** (Chart I) containing 1,10-phenanthroline (phen) and 2,9-

® Abstract published in *Advance ACS Abstracts*, November 15, 1993.

(1) (a) Trost, B. M.; Verhoeven, T. R. In *Comprehensive Organometallic Chemistry*; Wilkinson, G., Stone, F. G. A., Abel, E. W., Eds.; Pergamon: Oxford, U.K., 1982; Vol. 8, pp 799–938. (b) Consiglio, G.; Waymouth, R. M. *Chem. Rev.* **1989**, *89*, 257. (c) Godleski, S. A. In *Comprehensive Organic Chemistry*; Fleming, I., Ed.; Pergamon: Oxford, U.K., 1991; Vol. 4, pp 585–662.

(2) (a) Akermark, B.; Hansson, S.; Vitagliano, A. *J. Am. Chem. Soc.* **1990**, *112*, 4587. (b) Sjögren, M.; Hansson, S.; Norrby, P.-O.; Akermark, B.; Cucciolito, M. E.; Vitagliano, A. *Organometallics* **1992**, *11*, 3954.

(3) Vrieze, K. In *Dynamic Nuclear Magnetic Resonance Spectroscopy*; Jackman, L. M., Cotton, F. A., Eds.; Academic Press: New York, 1975.

(4) (a) Faller, J. W.; Thomsen, M. E.; Mattina, M. J. *J. Am. Chem. Soc.* **1971**, *93*, 2642. (b) Faller, J. W.; Tully, M. T. *J. Am. Chem. Soc.* **1972**, *94*, 2676.

(5) Oslinger, M.; Powell, J. *Can. J. Chem.* **1973**, *51*, 274–287.

(6) Crociani, B.; Di Bianca, F.; Giovenco, A.; Boschi, T. *Inorg. Chim. Acta* **1987**, *127*, 169–182.

(7) Albinati, A.; Kunz, R. W.; Ammann, C. J.; Pregosin, P. S. *Organometallics* **1991**, *10*, 1800–1806.

0276-7333/93/2312-4940$04.00/0

Chart I. Substituted (η^3-Allyl)palladium Phenanthroline Complexes[a]

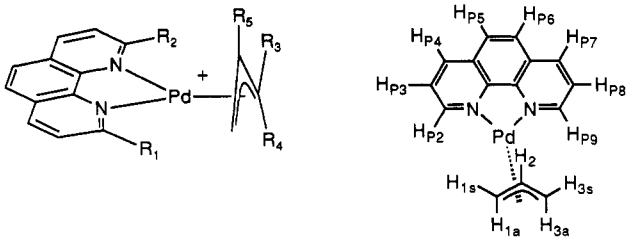

1a. R_1=R_2=R_3=R_5=H R_4=Me
1s. R_1=R_2=R_4=R_5=H R_3=Me
2a. R_1=R_2=R_4=Me R_3=R_5=H
2s. R_1=R_2=R_3=Me R_4=R_5=H
3. R_1=R_2=Me R_3=Ph R_4=R_5=H
4a. R_1=R_2=R_4=R_5=Me R_3=H
4s. R_1=R_2=R_3=R_5=Me R_4=H
5. R_1=R_5=H R_2=8-Methoxy-1-naphtyl R_3=R_4=D
6. R_1=R_2=R_3=R_4=Me R_5=H

[a] The numbering is for the unsubstituted complex. Notice the added index "P" for hydrogens on the phenanthroline ring.

dimethyl-1,10-phenanthroline (dmphen) as ancillary ligands, we noticed that the ligand methyl groups of complex **2** appeared as two singlets in the ^{1}H-NMR spectra, one each for the syn and anti isomers. At the time, it was not clear if this was due to fast exchange between the methyl groups of the two halves of the phenanthroline or to indistinguishable chemical shifts. In order to probe this, the phenyl-substituted allyl system **3** (counterion BF_4^-) was first studied. At 298 K, the two ligand methyl groups appeared as one broad singlet, but upon cooling of the sample to 200 K, they were split into two singlets separated by ca. 1 ppm. Saturation transfer between the two singlets confirmed that apparent rotation of the η^3-allyl (syn–syn, anti–anti exchange) was taking place. The coalescence temperature was ca. 270 K at 400 MHz. Upon addition of excess (ca. 30%) dmphen, saturation transfer indicated exchange between the free and complexed N–N ligand at 298 K, but upon cooling of the sample to 200 K, only the apparent rotation of the η^3-allyl group could be detected by saturation transfer. Thus it is clear that ligand exchange is slower than the apparent rotation. Exchange of the auxiliary phenanthroline ligand therefore is not involved in the apparent rotation. By contrast, addition of chloride ions (10 mol %), in the form of complex **3** with chloride counterion, resulted in an increase in the rate of the apparent rotation which is manifested as a lowering of the coalescence temperature from 270 to 200 K. This result supports the hypothesis that the apparent rotation is caused by pseudorotation in a 5-coordinate intermediate, because this is the only of the previously postulated mechanisms which involves a coordinating counterion. No other species could be detected at 200 K, showing that the exchange of chloride between complexes is a very fast process. It was noted that syn–anti exchange and exchange of the phenanthroline ligands were too slow to be detected by saturation transfer at 200 K even in the presence of chloride.

In a separate experiment, complex **3** (with BF_4^- as counterion) and excess dmphen was treated with $AgBF_4$ to remove possible traces of free chloride ions. Somewhat surprisingly, the coalescence temperature was still ca. 270 K suggesting a mechanism for apparent rotation which does not involve coordination of either chloride or free N–N ligand, in addition to the chloride-promoted process (see below).

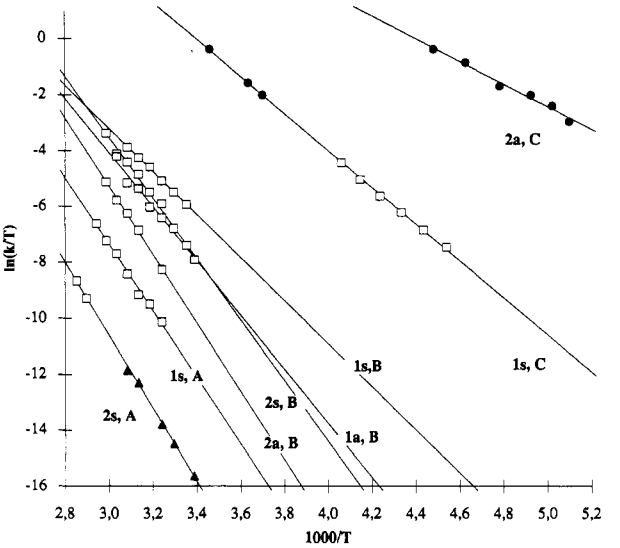

Figure 1. Eyring plots for the kinetic measurement runs on complexes **1** and **2**. The dynamic processes are defined as follows: (A) syn–anti isomerization; (B) syn–anti exchange of terminal protons; (C) apparent rotation of the allyl group. The techniques used are defined as follows: (□) saturation transfer; (●) coalescence; (▲) direct monitoring.

In order to investigate the syn–anti isomerization process, complex **4** (counterion BF_4^-), which is ca. 80% anti at equilibrium, was also studied. At 293 K, no syn–anti exchange processes could be detected by saturation transfer. The methyl groups on the ligand were equivalent, probably due to fast apparent rotation of the η^3-allyl. Upon addition of excess (ca. 30%) free dmphen, saturation transfer occurred only between the free ligand and the syn isomer **4s**. These experiments show that the balance between the exchange processes might be quite complicated and that the relative stability of the syn and anti isomers is important also in intermolecular exchange reactions. Therefore a detailed study of the rates and activation parameters for the various exchange processes was performed using the two model complexes **1** and **2** (Scheme I). The syn–anti exchange and isomerization were both studied in $CDCl_2CDCl_2$ solution, while for the apparent rotation 20:1 CD_2Cl_2/CD_3OD was used to permit measurements at low temperatures. The measurements were performed at 400 and 250 MHz with trifluoroacetate as counterion in the (η^3-allyl)palladium system.

Because of the large range of rates for the three processes studied (ca. 10^4–10^{-5} at 298 K), three different NMR techniques were used: coalescence, saturation transfer, and direct monitoring. The results are summarized in Figure 1.

The saturation-transfer technique is probably the least reliable of these because it can be affected by a fairly large systematic error due to incorrect estimation of relaxation rates and NOE contributions.[8] For the syn–anti proton exchange, the saturation transfer and the NOE are additive. To determine the NOE effects, the syn–anti proton exchange was "frozen out" at low temperature, and the remaining NOE effect was measured. The linear fit for three of the curves seems excellent. For the syn–anti-exchange in **1a** the fit was only satisfactory, due to the low relative abundance of this isomer. It is reassuring that for the two other processes, apparent allyl group rotation of

(8) Martin, M. L.; Delpuech, J. J.; Martin, G. J. In *Practical NMR Spectroscopy*; Heyden & Son Ltd.: London, 1980.

Scheme I. Isomerization and Proton-Exchange Processes[a]

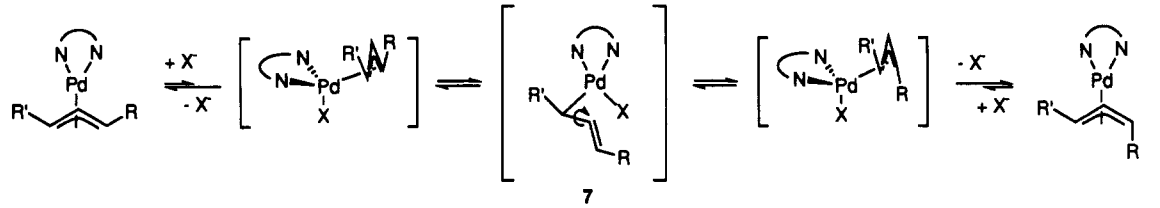

7

[a] The processes are defined as follows: R = Me, R′ = H, syn–anti isomerization; R = H, R′ = Me, syn–anti proton exchange.

Table I. Kinetic Constants and Activation Parameters for the Dynamic Processes of (1,10-Phenanthroline)- and (2,9-Dimethyl-1,10-phenanthroline)(crotyl)palladium Trifluoroacetate[a]

exchange process	complex	k_{298} (s^{-1})	$\Delta G^{\ddagger}_{298}$ (kJ/mol)	$\Delta H^{\ddagger}$ (kJ/mol)	$\Delta S^{\ddagger}$ (J/mol·K)
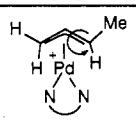	**1s** → **1a**	(2.8 ± 0.7) × 10^{-3}	87.6 ± 0.7	99 ± 8	38 ± 24
	2s → **2a**	(7.0 ± 0.7) × 10^{-5}	96.7 ± 0.2	109 ± 3	40 ± 9
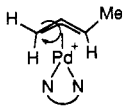	**1s**	0.78 ± 0.04	73.6 ± 0.1	64 ± 3	−32 ● 9
	1a	0.16 ± 0.08	77.5 ± 1.2	81 ± 19	10 ● 59
	2s	0.18 ± 0.03	77.2 ± 0.4	90 ± 7	44 ± 21
	2a	0.020 ± 0.005	82.7 ± 0.6	102 ± 7	64 ± 22
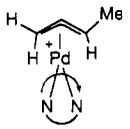	**1s**	396 ± 31	58.2 ± 0.2	55.0 ± 0.8	−10.6 ± 3.3
	1a[b]				
	2s[c]				
	2a	(2.1 ± 1.6) × 10^{4}	48 ± 2	33 ± 4	−50 ± 21

[a] Error limits are at 90% confidence limits. All values are calculated with the assumption that $\Delta C_p^{\ddagger} = 0$. Possible errors in NOE estimation are not included in the confidence limits. [b] Not detected (overlapped weak signals). [c] Not detected (too fast).

1s and the syn–anti isomerization of **2s**, the rates determined by saturation-transfer data fall nicely on the straight line obtained from one other method (see Figure 1). This gives some extra credence to the values for $\Delta H^{\ddagger}$ and $\Delta S^{\ddagger}$ determined from the former method.

Syn–Anti Isomerization and Syn–Anti Proton Exchange. As might be expected, the syn–anti isomerization is the slowest of the studied processes.[9] By saturation-transfer measurements involving the allyl methyl groups of the two isomers at temperatures between 308 and 340 K, first-order rate constants in the range 0.01–0.45 s^{-1} were obtained for the isomerization **1s** → **1a** (Table I and Figure 1). This can be extrapolated to a rate of 2.8 × 10^{-3} s^{-1} at 298 K. Because an equilibrium is established where the ratio for **1s**/**1a** is 10/1, the corresponding rate for the reverse reaction **1a** → **1s** is 10 times as high. In the case of the complex **2**, the syn–anti isomerization is considerably slower. For the reaction **2s** → **2a**, saturation transfer was measured at 345 and 350 K. Because syn–anti isomerization is slow for this complex, the pure syn and anti isomers could be isolated.[10] The isomerization of the complex **2s** therefore could be monitored directly at temperatures between 295 and 324 K. The results from the two methods agree very well, permitting a reliable determination of the activation parameters (Table I and Figure 1). The rates are 7 × 10^{-5} s^{-1} at 298 K for **2s** → **2a** and 3.5 × 10^{-5} s^{-1} for **2a** → **2s** (**2s**/**2a** = 1/2 at equilibrium).

The syn–anti proton exchange, which like the syn–anti isomerization must proceed via a η^3–η^1–η^3 rearrangement, should be affected similarly by the ligands. This is largely in accordance with the experimental results except that the negative activation entropy, which would be anticipated for an associative process, in fact is observed for the syn–anti exchange in **1s**. In the temperature range where rates could be measured conveniently by saturation transfer, the rates for syn–anti proton exchange were higher for the complex **1** than for the complex **2**. The rates are also higher for the syn than for the anti isomers. For example, at 309 K the ratios **1s**:**2s**:**1a**:**2a** are 22:10:6:1. Extrapolation to higher temperatures (Figure 1) indicates that the exchange rate in complex **2s** should become faster than in complex **1s** at temperatures around 360 K. In order to verify this, attempts were made to obtain coalescence data. Because of the slow syn–anti isomerization, it was possible to observe coalescence for the syn–anti proton exchange for **1s** at 356 K. Unfortunately, this result was not reliable because some type of decomposition at this temperature gave small amounts of an unidentified species that catalyzed the syn–anti exchange. This could be observed as a continuous decrease in the coalescence temperature when the NMR sample was repeatedly heated and then cooled.

The dependence of syn–anti isomerization and syn–anti proton exchange on the counterion was investigated by saturation-transfer experiments on complex **1** at constant total concentration but with different relative amounts of chloride and trifluoroacetate counterions. The rates of both processes were found to increase monotonously when going from pure trifluoroacetate complex to successively higher amounts of chloride. The syn–anti proton exchange became too fast to be measured by saturation transfer at about 10% chloride. At 6% chloride, the geminal allyl protons had undergone *J*-coalescence, transforming H_2 in the allyl from an apparent doublet of triplets to an apparent quartet. This uniform coalescence also shows that all molecules in solution experience the acceleration from the chloride; therefore, the exchange of chloride between complexes must be very fast. The

(9) Maitlis, P. M.; Espinet, P.; Russel, M. J. H. In *Comprehensive Organomeallic Chemistry*; Wilkinson, G., Stone, F. G. A., Abel, E. W., Eds.; Pergamon: Oxford, U.K. 1982; Vol. 6, pp 419.

(10) Vitagliano, A.; Akermark, B.; Hansson, S. *Organometallics* **1991**, *10*, 2592.

characteristic NOE between the phenanthroline and the allyl moieties, as well as the coupling constants, remained essentially unchanged at all concentrations of Cl (0–100%), suggesting that the major isomer was always the square planar η^3-allyl complex. The saturation transfer between syn and anti isomer was similar in the allyl and phenanthroline moieties, indicating that the ligand exchange rate is negligible compared to even the slowest of the dynamic processes studied here.

The absolute concentration dependence of the processes was also tested in separate saturation-transfer experiments. When complex **1** was used with trifluoroacetate counterion, only the syn–anti proton exchange was fast enough to be studied by saturation transfer at ambient temperature. Dilution of the sample to half the normal concentration had no appreciable effect on the measured saturation transfer. In **1** with chloride as counterion, the syn–anti isomerization can be conveniently measured by an intermediate saturation transfer, and the syn–anti proton exchange is manifested as an extensive line broadening of H_{1a} and H_{1s}. Both the saturation transfer and the line broadening were constant upon dilution of the sample to half the normal concentration. These results indicate that the processes are first order in complex and that the complex is present as an ion pair in solution, not as separate ions.

In accordance with earlier studies,[3] the results obtained can be rationalized by the reactions outlined in Scheme I. Starting from the η^3-allyl complex, the entropy must clearly decrease when going to the 5-coordinate species. However, formation of the η^1-allyl complex **7** involves breaking a π-bond to palladium and should increase the entropy of the system. The entropy change in going from η^3-allyl complex to **7** is not obvious; it should depend both upon how tightly the counterion is held in the η^3-allyl complex and how hindered rotation is in complex **7**, but the positive values in the majority of the reactions (well within the 90% confidence limits in most cases) can easily be explained by a tightly held counterion. The trend in the enthalpies are most easily described by comparison between complexes **1** and **2**. The ligand methyl groups in **2** should destabilize the η^3-allyl complex, have little effect upon the 5-coordinate complex (*cf.* the X-ray structure below), and strongly destabilize the η^1-allyl complex of type **7**. Complex **7** is more sterically crowded and should therefore be more destabilized than the η^3-allyl complex because of the larger substituent angle (C–Pd–C in **2** is $\approx$70°; C–Pd–X in **7** is expected to be $\approx$90°). The crowding should be most severe when the carbon binding to palladium is secondary, as in the syn–anti isomerization. This is in complete accordance with the results in Table I. The processes expected to go through complexes of type **7** have higher activation enthalpies for **2** than for **1**. The syn–anti isomerization has a higher activation enthalpy than the syn–anti proton exchange. The activation enthalpy for the syn–anti proton exchange is also higher for anti complexes than for syn complexes, because rotation around the C–C single bond in the η^1-allyl complex is more hindered.

One entry, the syn–anti proton exchange in **1s**, deserves some extra notice. The entropy of activation is negative here, which indicates that the rate-determining step has changed. As indicated above, the formation of a 5-coordinate intermediate should be less facile for **1** than for **2**. Additionally, the η^1-allyl complex, which is the supposed intermediate in syn–anti proton exchange in **1s**, should be the least crowded of the six possible intermediates of type **7**. Together, these observations make it very plausible that the association of complex and counterion has become rate determining in this case. On the other hand, if formation of the 5-coordinate intermediate was completely rate determining, the activation parameters should be the same as for the apparent rotation in **1s** (see below). The trend is right (a lowering of both activation enthalpy and entropy compared to the other η^3–η^1–η^3 processes), but the parameters clearly are not identical. However, if the formation of the 5-coordinate intermediate is not completely rate determining in the syn–anti proton exchange of **1s**, the rates of formation and further reaction of this intermediate should be similar, and therefore the overall activation parameters will include contributions from both transition states.

The influence of solvent and counterion on the relative rates of syn–anti isomerization supports the assumed mechanism. When the complex **2s** [BF_4^-] was prepared from the chloride complex using excess (ca. 20%) $AgBF_4$ to trap all chloride, a complex which was inert toward isomerization at 298 K was obtained. At 333 K, the isomerization was slow ($k \approx 10^{-5}$ s^{-1}). In contrast, addition of 4 mol % chloride ions (as **2s** with chloride counterion) led to very fast isomerization, which even at 298 K was complete within a few minutes. It was also found that change of solvent from $CDCl_2CDCl_2$ to D_2O led to a decrease of the isomerization rate of **2s** ($CF_3CO_2^-$ counterion) by approximately 2 orders of magnitude at 333 K. A reasonable explanation is that water stabilizes the cationic 4-coordinate η^3-allyl complex by efficient solvation of the ions, thereby decreasing the rate of isomerization. This is also in complete accordance with our earlier observation that the complex **2s**, with chloride counterion, is nonconducting in dichloromethane but conducting in water.[2b]

The dependence of the relative rates of syn–anti isomerization and syn–anti exchange on the counterion clearly is of interest in relation to catalytic reactions involving η^3-allyl intermediates. The influence of syn–anti exchange is subtle because it will only result in a switch of the chirality of the allyl group. Therefore this can be important in chiral induction and can be detected as an exchange between diastereomeric complexes, for instance the process (S_p,R_a)-**5a** $\rightarrow$ (R_p,R_a)-**5a** as discussed below.

In contrast, syn–anti isomerization can be used in principle to control the Z/E ratio in the products from allylic substitution. The counterion will be very important. If allyl acetates are substrates, it will be expected that isomerization of the intermediate η^3-allyl complexes will be more rapid than when trifluoroacetates are used. Moreover, an excess of counterion will be present during catalytic conditions, further increasing the isomerization rate compared to the case of isolated complexes. However, it seems probable that the relative effects of the N–N ligand on the different exchange processes will be approximately the same. Thus it should be possible to extrapolate from the results with trifluoroacetate to other systems. In fact, the results from experiments with catalytic displacement of acetate in *E*- and *Z*-2-hexenyl acetate by diethyl methylmalonate anion are illustrative. When the phen complex **1** is used as catalyst, both acetates give a 10/1 mixture of *E*- and *Z*-products, while, with the dmphen complex **2**, complete retention of stereochemistry is

observed.[11] This shows that the syn–anti isomerization is faster than nucleophilic attack with the complex **1** but slower with complex **2**. Thus subtle control of the stereochemistry of the products from palladium-catalyzed allylic substitution is possible by steric modification of ligands of the phenanthroline type.

Apparent Rotation of the Allyl Group. The apparent rotation is the fastest of the exchange processes studied here. The phen complex **1** at 298 K showed broadened signals for the phen protons, which upon cooling to 253 K appeared as two sets of signals corresponding to the two halves of the phenanthroline ligand. Two coalescence temperatures could be determined for the most abundant isomer **1s** at 400 MHz, H_{P3} and H_{P8} at 275 K ($\Delta\nu$ = 26 Hz) and H_{P2} and H_{P9} at 289 K ($\Delta\nu$ = 90 Hz). The ^{13}C-spectrum yielded one more coalescence, C_{P3} and C_{P8} at 270 K ($\Delta\nu$ = 16.5 Hz). The Eyring plot shows a remarkable consistency between the rates determined by coalescence and saturation transfer and permitted an accurate evaluation of the activation parameters. Because of an overlapping weak signal, the rate parameters could not be determined for the minor isomer **1a**.

In the case of complex **2**, the apparent rotation was fast even at 183 K for the syn isomer **2s** (only broadening of the dmphen methyl signal was observed at this temperature), while, for **2a**, the methyl group protons and some of the aromatic carbons (by ^{13}C NMR) gave two separate signals. Six coalescence temperatures could be determined, H_{P2Me} and H_{P9Me} at 209 K ($\Delta\nu$ = 18 Hz), C_{P13} and C_{P10} at 196 K ($\Delta\nu$ = 4.7 Hz), C_{P11} and C_{P12} at 199 K ($\Delta\nu$ = 8.3 Hz), C_{P4} and C_{P7} at 203 K ($\Delta\nu$ = 12.7 Hz), C_{P2Me} and C_{P9Me} at 216 K ($\Delta\nu$ = 43 Hz), and C_{P2Me} and C_{P9Me} at 223 K ($\Delta\nu$ = 70.7 Hz) (Figure 1 and Table I). It is interesting to note that the apparent rotation is much faster for complex **2** than for complex **1**, with an activation energy difference larger than 20 kJ mol^{-1}. It is also interesting to note that the processes have a negative entropy of activation which is considerably larger for the dmphen complex **2a**. Although the sign of the activation entropy may be uncertain for **1s**, this suggests that both processes are associative and presumably involve a 5-coordinate intermediate.

By assuming a pentacoordinate intermediate, the higher rate of the apparent rotation in the dmphen complex is explained and consistent with pseudorotation for such an intermediate.[12] This conclusion is supported further by experiments using different counterions with the (η^3-allyl)-palladium system **2a**. With the fairly noncoordinating BF_4^- counterion, coalescence of the protons on the two methyl groups was observed at 240 K as compared to 210 K with the moderately coordinating trifluoroacetate counterion (5:1 $CDCl_3$:CD_3NO_2; 400 MHz). This corresponds to a difference in $\Delta G^{\ddagger}$ of ca. 6 kJ/mol. With the more strongly coordinating chloride ion, addition of only 10 mol % to the trifluoroacetate complex led to such a large acceleration of the apparent rotation such that no splitting of the methyl resonances was detected even as low as 183 K.

(11) Sjögren, M. P. T.; Hansson, S.; Akermark, B.; Vitagliano, A. Manuscript in preparation.

(12) The 5-coordinate adduct would be more stable (compared with the cationic starting complex) in the case of dmphen, due to the loss of the steric interaction between the dmphen methyl groups and the terminal allyl carbons. It is interesting to note that the observed difference of about 10 kJ/mol between the activation free energies of the two complexes compares well with the stability difference (ΔG° = 12 kJ/mol) between the corresponding propenyl complexes, which we have directly measured through ligand-exchange experiments.

Scheme II. Exchange Processes Observed for Complex 5[a]

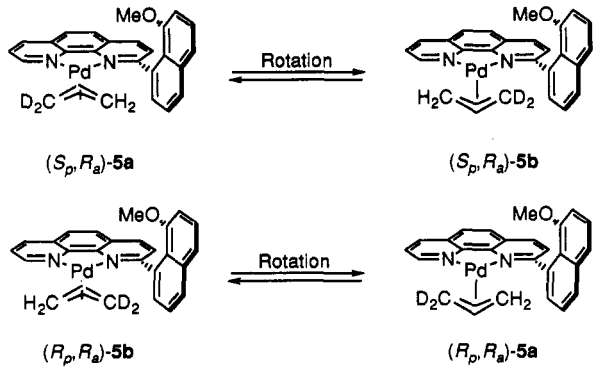

[a] For clarity only one set of enantiomers is shown.

As observed earlier, exchange of the phen and dmphen ligands, respectively, was negligible for complexes **1** and **2**. This conclusion is based on the absence of ligand exchange between the syn and anti isomers in the temperature range 298–338 K, where very fast apparent rotation is observed.

Although it would appear that pseudorotation within a 5-coordinate complex is the most probable mechanism for apparent rotation, a mechanism involving palladium(0)-catalyzed allyl exchange could not be excluded. Because traces of palladium(0) could form readily in reactions with allyl systems, it can be imagined that it can act as a nucleophile and react with (η^3-allyl)palladium complexes, displacing the initially bound palladium.[13] The result of this process is a flip of the allyl group (e.g. (S_p,R_a)-**5a** → (R_p,R_a)-**5a**). In order to study this possibility, the racemic complex **5** was prepared (BF_4^- as counterion). Due to the chirality of the ligand, four diastereomeric complexes are possible. Molecular mechanics calculations[14] indicate that even though the free ligand can exchange between its enantiomers by rotation of the naphthyl, this exchange is not possible in the complex. An apparent rotation (a true rotation or a pseudorotation) would give pairwise exchange as depicted in Scheme II. If η^3–η^1–η^3 isomerization is slow, ligand exchange will not affect the configuration of the η^3-allyl moiety whereas the configuration of the ligand is scrambled. This gives an exchange of allyl protons between all four diastereomeric forms, albeit not the (undetectable) exchange between enantiomeric forms. In contrast, nucleophilic displacement of ligated palladium by palladium(0), presumably coordinated to at least one phenanthroline ligand, will lead to inversion of the configuration of the allyl group. All different diastereomers and enantiomers will thus exchange, including e.g. (S_p,R_a)-**5a** and (R_p,R_a)-**5a** in Scheme II. Because all four sets of terminal allyl protons are resolved in the NMR spectrum of **5** at ambient temperature, it can be shown that only the pairwise exchange according to Scheme II takes place, excluding the alternative displacement by palladium(0) or free ligand in this system.

It was also possible to make a tentative assignment of the protons to the four different diastereomers. This is based on the assumption that the protons for the isomers **5a** correspond to high-field protons at ca. 2 ppm due to shielding effects from the methoxynaphthyl group. On

(13) Granberg, K. L.; Bäckvall, J. E. *J. Am. Chem. Soc.* **1992**, *114*, 6858.

(14) MacMimic/MM2(91) for Macintosh, InStar Software AB, IDEON Research Park, S-223 70 Lund, Sweden.

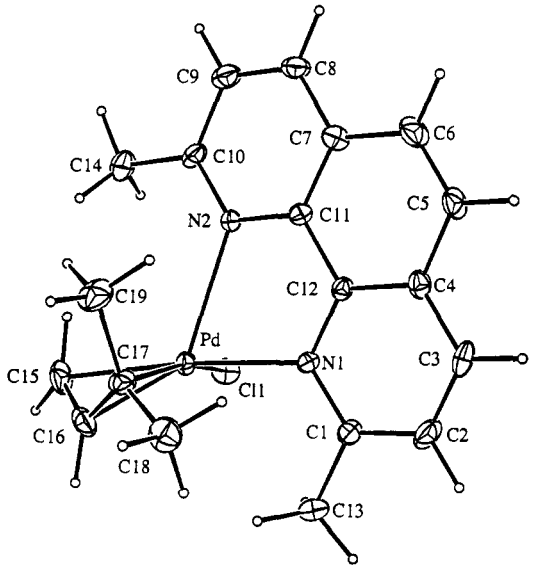

Figure 2. ORTEP view of the complex **6** showing the atom-labeling scheme. Thermal ellipsoids are drawn at the 25% probability level.

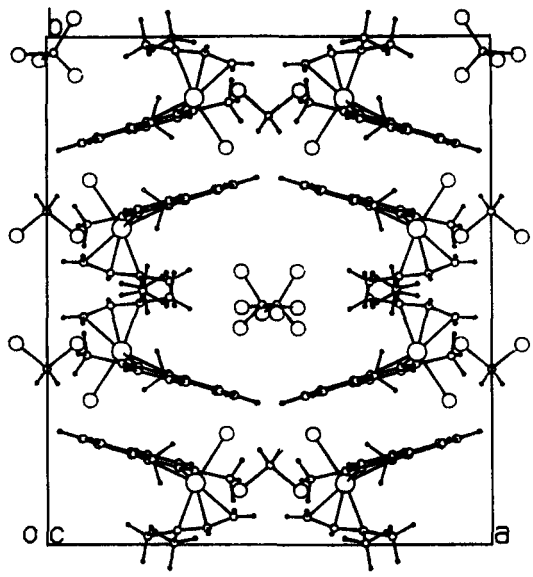

Figure 3. Crystal packing of complex **6** as viewed along the *c* axis.

the basis of the further assumption that the syn-proton (and the central proton) is more shielded in (S_p,R_a)-**5a** (and (R_p,R_a)-**5a**) than in (R_p,R_a)-**5a** (and (S_p,S_a)-**5a**), all allyl protons could be assigned to one diastereomer. It could then be shown that each terminal proton shows saturation transfer only to one proton in one of the other diastereomers, in accordance with Scheme II. This rules out both nucleophilic displacement by palladium(0) and ligand exchange as responsible for the apparent rotation, in accordance with direct measurements of ligand exchange as described above. Together with the accelerating effect of chloride ion as shown for **2** and **3**, this is strong support for a mechanism for apparent rotation which proceeds via a 5-coordinate intermediate. An interesting observation is that the ratios between the two sets of isomers ((S_p,R_a)-**5a** + (R_p,R_a)-**5b**)/((S_p,R_a)-**5b** + (R_p,R_a)-**5a**) is different from 1 (≈1.2). In principle, this amounts to chiral induction in an unsubstituted η^3-allyl system and indicates the potential of the substituted phenanthrolines as chiral ligands.

It may be mentioned that for rigid ligands such as the 1,10-phenanthrolines, it may be difficult to distinguish apparent rotation via a 5-coordinate intermediate and one involving dissociation of one nitrogen, rotation, and recombination[15] as proposed by Pregosin et al.[7] In fact, the difference between a monodentate and a chelating phenanthroline may be quantitative rather than qualitative. Even the nonbonded nitrogen in the former case would be closer to palladium (ca. 2.7 Å) than the sum of the Van der Waals radii (ca. 3.3 Å). It turns out that the structure of dmphen complex **6** is quite informative.

Molecular Structure of (2,9-Dimethyl-1,10-phenanthroline)[(1,2,3-η)-3-methyl-2-butenyl]chloropalladium (6). The structure of the title compound is shown in Figure 2. The crystal contains discrete molecules of the complex and clathrated methylene chloride and carbon tetrachloride in a 1:0.5:0.5 ratio (Figure 3). The refined atomic parameters are listed in Table II, and relevant bond lengths and angles are reported in Table III.

Table II. Fractional Atomic Coordinates and Equivalent Isotropic Thermal Parameters (Å²) of the Non-Hydrogen Atoms with Their Estimated Standard Deviations in Parentheses

	x	*y*	*z*	B_{eq}[a,b]
Pd	0.66805(3)	0.12106(3)	0.65479(5)	2.14(1)
Cl(1)	0.5967(1)	0.2172(1)	0.5734(2)	3.14(4)
N(1)	0.7744(3)	0.1660(3)	0.7242(5)	2.1(1)
N(2)	0.7046(3)	0.1519(3)	0.8824(6)	2.1(1)
C(1)	0.8069(4)	0.1777(4)	0.6453(7)	2.7(2)
C(2)	0.8790(4)	0.1990(5)	0.6921(8)	3.7(2)
C(3)	0.9193(4)	0.2074(5)	0.8237(9)	3.6(2)
C(4)	0.8852(4)	0.1963(4)	0.9049(8)	2.5(2)
C(5)	0.9220(4)	0.2073(5)	1.0395(9)	3.2(2)
C(6)	0.8884(5)	0.2002(5)	1.1178(9)	3.7(2)
C(7)	0.8134(4)	0.1817(4)	1.0668(7)	2.7(2)
C(8)	0.7747(5)	0.1770(4)	1.1432(7)	2.9(2)
C(9)	0.7040(5)	0.1600(4)	1.0903(8)	3.2(2)
C(10)	0.6689(4)	0.1473(4)	0.9566(7)	2.6(2)
C(11)	0.7757(4)	0.1690(4)	0.9364(7)	2.2(2)
C(12)	0.8120(4)	0.1768(4)	0.8524(7)	2.0(1)
C(13)	0.7639(5)	0.1680(5)	0.5040(8)	4.0(2)
C(14)	0.5908(4)	0.1290(5)	0.8957(9)	3.7(2)
C(15)	0.5812(5)	0.0548(5)	0.5853(9)	3.9(2)
C(16)	0.6417(5)	0.0327(4)	0.5689(9)	3.4(2)
C(17)	0.7089(4)	0.0266(4)	0.6754(7)	2.8(2)
C(18)	0.7758(5)	0.0154(5)	0.6541(9)	4.2(2)
C(19)	0.7156(6)	0.0027(5)	0.8045(9)	4.5(2)
C(20)	0.5	0.1541(7)	0.25	3.9(3)
Cl(2)	0.4315(1)	0.1066(2)	0.2628(3)	5.7(1)
C(21)	0.517(2)	0.470(2)	0.472(3)	23(3)*
Cl(3)	0.4371(6)	0.4646(6)	0.495(1)	23(1)*
Cl(4)	0.566(1)	0.422(1)	0.593(2)	23(1)*
Cl(5)	0.485(1)	0.452(1)	0.334(2)	25(1)*

[a] $B_{eq} = {}^4/_3\sum_i\sum_j\beta_{ij}a_ia_j$. [b] Note: The atoms C(20), C(21), Cl(4), and Cl(5) have been refined with an occupancy factor of 0.5. Starred *B* values are for atoms that were refined isotropically.

The most relevant feature of the structure is the unusual coordination stereochemistry displayed by the Pd(II) center. The geometry of the complex is probably best described as distorted square pyramidal, with the terminal allyl carbons (C(15) and C(17)), the chloride ion (Cl(1)), and one nitrogen (N(1)) occupying the basal sites and the second nitrogen (N(2)) occupying the apical site. While the allyl group is symmetrically bound (Pd–C(15) =

(15) The distinction is actually possible in the case of flexible ligands, such as tetramethylethanediamine (TMEDA). During previous work with this ligand (unpublished results) we have observed an apparent rotation of the crotyl group, which resulted in a pairwise coalescence between methyl groups on different nitrogens, but no exchange between methyls on the same nitrogen. This indicates that the exchange mechanism did not involve the dissociation of one nitrogen atom, since if this would have been the case, the fast nitrogen inversion occurring after dissociation would have scrambled all four methyl groups.

Scheme III. Proposed Mechanism for the Apparent Rotation of (η^3-Allyl)palladium Phenanthroline Complexes

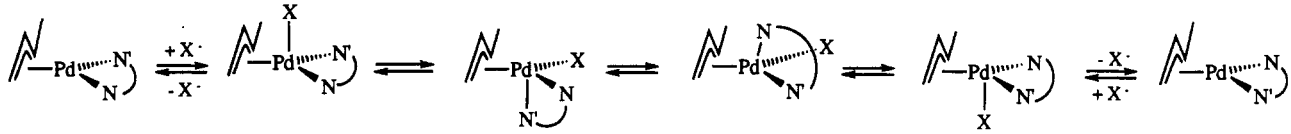

Table III. Bond Lengths (Å) and Relevant Valence Angles (deg) with Their Estimated Standard Deviations in Parentheses[a]

Bond Lengths			
Pd–Cl(1)	2.451(3)	Pd–C(16)	2.09(1)
Pd–C(15)	2.13(1)	Pd–C(17)	2.15(1)
Pd–N(1)	2.17(1)	Pd–N(2)	2.49(1)
C(15)–C(16)	1.39(2)	C(16)–C(17)	1.40(2)
C(17)–C(18)	1.49(2)	C(17)–C(19)	1.52(2)
N(1)–C(1)	1.35(1)	N(2)–C(10)	1.33(1)
N(1)–C(12)	1.37(1)	N(2)–C(11)	1.35(1)
C(4)–C(12)	1.40(1)	C(7)–C(11)	1.39(1)
C(3)–C(4)	1.39(2)	C(7)–C(8)	1.40(2)
C(2)–C(3)	1.40(2)	C(8)–C(9)	1.34(2)
C(1)–C(2)	1.40(2)	C(9)–C(10)	1.42(2)
C(1)–C(13)	1.50(2)	C(10)–C(14)	1.48(2)
C(4)–C(5)	1.43(2)	C(6)–C(7)	1.43(2)
C(11)–C(12)	1.45(1)	C(5)–C(6)	1.34(2)
C(21)–Cl(3)	1.74(4)	C(21)–Cl(13)*	1.63(4)
C(21)–Cl(4)	1.67(4)	C(21)–Cl(5)	1.49(4)
C(20)–Cl(2)	1.77(1)		
Bond Angles			
Cl(1)–Pd–N(1)	96.0(2)	Cl(1)–Pd–N(2)	92.8(2)
Cl(1)–Pd–C(15)	98.6(3)	Cl(1)–Pd–C(16)	125.3(3)
Cl(1)–Pd–C(17)	163.8(3)	N(1)–Pd–N(2)	71.7(2)
C(15)–Pd–C(16)	38.6(4)	C(16)–Pd–C(17)	38.6(4)
C(15)–Pd–C(17)	68.9(4)	N(2)–Pd–C(16)	129.7(3)
N(1)–Pd–C(15)	164.0(4)	N(1)–Pd–C(17)	95.6(3)
C(16)–C(17)–C(18)	119.1(9)	C(16)–C(17)–C(19)	122.8(9)
C(15)–C(16)–C(17)	119.8(9)		

[a] Note: Cl(3)* is related to Cl(13) by the symmetry operation $1-x$, $1-y$, $1-z$.

2.13(1) Å and Pd–C(17) = 2.15(1) Å), the dmphen ligand is unsymmetrically bound, the apical Pd–N(2) distance (2.49(1) Å) being much longer than the basal Pd–N(1) distance (2.17(1) Å). The weak Pd–N(2) bond is actually intermediate between a normal bond (like Pd–N(1)) and a long-range interaction like that found in "monodentate" phenanthroline complexes.[16] Accordingly, the stereochemistry of the complex could be viewed as intermediate between the square-planar geometry and a square-pyramidal geometry. In the former case the palladium atom should be virtually coplanar with the baricenter of the allyl triangle and the two remaining ligands, while in the latter case the palladium atom should ideally be displaced ≈0.4 Å above that plane toward the apical ligand.[17] Actually, in the case of complex **6**, the palladium atom is displaced 0.257(1) Å above the plane defined by Cl(1), N(1), and the baricenter of the allyl triangle. A geometrically similar arrangement of the dmphen ligand has been recently found in a five-coordinate carbonyl complex of platinum(II).[16b]

Apart from the above considerations, all the other bond distances and angles in the molecule fall within the expected range. The plane of the dmphen ligand (maximum atomic out-of-plane displacement: 0.09(1) Å) displays a slight but significant convexity. As usual for η^3-allyl complexes,[18] the allyl triangle forms a dihedral angle of 106.5(8)° with the plane defined by its baricenter and by N(1) and Cl(1). The two methyl groups C(18) and C(19) are displaced by 0.27(1) and 0.81(1) Å from the allyl plane toward the metal and away from the metal, respectively.

The structural features of complex **6** give strong support to the pseudorotation in a five-coordinate intermediate as the operating mechanism for the apparent rotation of the allyl group. Indeed, **6** looks quite similar to one of the intermediates in the chain of intramolecular movements ultimately leading to the site exchange of coordinated nitrogen atoms in the cationic allyl complex (Scheme III).

It is worth noting that, in contrast to the structure of square-planar cationic η^3-allyl complexes of dmphen,[19] no steric constraints are found in the structure of **6**. As anticipated previously, the methyl substituents on the dmphen ligand are far apart from any of the other ligand atoms (closest contact larger than 3.6 Å). This observation provides good support for the explanation given before for the lower barrier to the apparent rotation found in dmphen complexes compared to phen analogs.

Conclusions

The results reported above can be rationalized by considering that the use of 2,9-disubstituted phens destabilizes the square-planar geometries containing the N–N ligand in the coordination plane. This implies that processes involving a square-planar species as a transition state (*e.g.* the η^3–η^1–η^3 rearrangement) are *disfavored*, while processes involving a pentacoordinate intermediate (*e.g.* the apparent rotation of the allyl group) are *favored*.

As a consequence, the occurrence of the allyl inversion (through a η^3–η^1–η^3 mechanism) or syn–anti isomerization during a catalytic nucleophilic substitution could possibly be produced or avoided by simply switching from unsubstituted phen to a 2,9-disubstituted 1,10-phenanthroline is ancillary ligand, a hypothesis that we have already tested in the case of syn–anti isomerization.[11]

A second possible implication, which we have not tested yet, is that 2,9-disubstituted phenanthrolines might improve the reactivity in the addition of "hard" nucleophiles to η^3-allyl system, by facilitating the precoordination of the nucleophile in a five-coordinate intermediate.

In summary, the results presented in this paper give an illustration of the potential of phenanthroline ligands for the modulation of reactivity in allyl–palladium chemistry.

Experimental Section

^{1}H NMR spectra were recorded on 400-MHz (Bruker Model AM400) and 250-MHz (Bruker Model ACF250) instruments. ^{1}H NMR chemical shifts are reported in δ (ppm) relative to Me_4Si as internal standard. ^{1}H NMR integrations are reported as relative number of hydrogens (H). Because of the straightforward

(16) (a) Dixon, K. R. *Inorg. Chem.* **1977**, *16*, 2618. (b) Fanizzi, F. P.; Maresca, L.; Natile, G.; Lanfranchi, M.; Tiripicchio, A.; Pacchioni, G. *J. Chem. Soc., Chem. Commun.* **1992**, 333.

(17) Preston, H. S.; Kennard, C. H. L. *J. Chem. Soc. A* **1969**, 2682.

(18) Lippard, S. J.; Morehouse, S. M. *J. Am. Chem. Soc.* **1972**, *94*, 6956.

(19) Eriksson, L.; Sjögren, M. P. T.; Akermark, B. Manuscript in preparation.

method used in the preparation of the complexes, ^{1}H NMR data were assumed generally sufficient for full characterization of the compounds. All 1,10-phenanthroline derivatives were purified by medium-pressure liquid chromatography (MPLC) as described by Baeckström et al.[20] The gel used was Merck aluminum oxide (basic) and the solvent gradient was a mixture of CH_2Cl_2 and hexane. TLC analysis was performed on Merck aluminum-backed F_{254} aluminum oxide (neutral) plates using UV light for visualization. Melting points were determined in open capillary tubes and are uncorrected.

Materials. (1,10-Phenanthroline)[(1,2,3-η)-2-butenyl]palladium trifluoroacetate (1),[10] (2,9-dimethyl-1,10-phenanthroline)-[(1,2,3-η)-2-butenyl]palladium trifluoroacetate (2),[10] (2,9-dimethyl-1,10-phenanthroline)[(1,2,3-η)-1-phenyl-2-propenyl]palladium tetrafluoroborate (3),[2b] (2,9-dimethyl-1,10-phenanthroline)-[(1,2,3-η)-2-methyl-2-butenyl]palladium tetrafluoroborate (4),[10] bis(μ-chloro)bis[(1,2,3-η)-3-methyl-2-butenyl]palladium (5),[21] 1,1-dideutero-2-propen-1-ol,[22] and (1-methoxynaphth-8-yl)lithium[23] were prepared as described in the literature. All other chemicals were purchased from Aldrich and purified and dried with standard methods.[24]

Kinetic Measurements. The dynamical processes were all investigated by ^{1}H and/or ^{13}C NMR spectroscopy at the same concentration of 0.050 mol/L in the appropriate solvent. A 95:5 mixture of CD_2Cl_2:CD_3OD was used in the low-temperature range (methanol was needed to improve the solubility of the complexes), while $CDCl_2CDCl_2$ was used at room and high temperature. The temperature was calibrated using a separate methanol sample. The rates were determined over a temperature range of at least 30 °C by one or two of the following techniques: (i) Measurement of the *coalescence temperature* of a pair of exchanging nuclei was performed. In this case the rate was simply calculated from the equation $k = \pi\Delta\nu/\sqrt{2}$. No line shape analysis was performed. Rather, several coalescence phenomena occurring at different temperatures, involving different pairs of exchanging nuclei were observed. (ii) *Saturation-transfer experiments* were completed. These were performed under steady-state conditions using a standard program for NOE difference spectroscopy with a pre-irradiation time of 5 s. The fractional change of the observed magnetization of nucleus a upon irradiation of nucleus b (f^b) was evaluated in the difference spectrum by integration of the residual signals due to nuclei b and a. A change of ±2 s in the pre-irradiation time did not cause any appreciable change in f^b. The exchange rate for the process a → b was evaluated by the equation[8] $k_1 = R_a(-f^b + \eta)/(K + f^b)$, where K is the equilibrium ratio a/b, R_a is the apparent relaxation rate of nucleus a, and η is the NOE enhancement factor due to cross-relaxation between b and a. R_a was independently estimated through linear interpolation of the values obtained by standard inversion-recovery experiments, run at the extremes of the temperature interval of interest. The NOE enhancement was appreciable only when the geminal allyl protons were the exchanging nuclei.[25] It was estimated to be the residual fractional change of magnetization f^b measured at the limit of $k_1 \ll R_a$ (low temperature) and was assumed to be constant over the temperature range involved. Secondary NOE effects (multiple cross-relaxation) were neglected.

2-(8-Methoxy-1-naphthyl)-1,10-phenanthroline. This compound was prepared in accordance with a method described in the literature.[26] To a stirred suspension of 1,10-phenanthroline (1.44 g, 8 mmol) in anhydrous toluene (28 mL), (1-methoxynaphth-8-yl)lithium (5.3 g, 32 mmol) dissolved in anhydrous THF (50 mL) was added dropwise (30 min) under nitrogen. The mixture was stirred at room temperature for 18 h, after which water (30 mL) was added at 0 °C. The organic phase was separated, the aqueous phase was extracted two times with methylene chloride (30 mL), and the organic fractions were combined. MnO_2 (50 g) was added, and the mixture was stirred for 30 min. After addition of anhydrous magnesium sulfate (50 g) and additional stirring for 30 min, the mixture was filtered, and the filtrate was concentrated on the rotary evaporator. Excess 1-methoxynaphthalene was removed with a bulb to bulb distillation apparatus at 0.05 mmHg at 100 °C for 2 h. The crude product then was purified by MPLC, and 1.35 g (50%) of light brown product was isolated. Recrystallization from hot chloroform gave analytically pure product as light yellow crystals, mp 123–124 °C. ^{1}H NMR (250 MHz, $CDCl_3$): δ 9.19 (dd, J = 4.2 Hz, J = 1.5 Hz, 1 H), 8.19 (dd, J = 8.0 Hz, J = 1.5 Hz, 1 H), 8.12 (d, J = 8.3 Hz, 1 H), 7.88 (br d, J = 8.0 Hz, 1 H), 7.82 (d, J = 8.7 Hz, 1 H), 7.74 (d, J = 8.7 Hz, 1 H), 7.67–7.49 (m, 5 H), 7.38 (t, J = 8.0 Hz, 1 H), 6.72 (d, J = 7.5 Hz, 1 H), 3.30 (s, 3 H). ^{13}C NMR (62 MHz, $CDCl_3$): δ 163.3, 156.0, 150.0, 146.3, 144.6, 137.8, 135.7, 135.2, 133.1, 129.0, 128.5, 128.2, 126.6, 126.2, 125.7, 125.5, 125.3, 125.0, 123.2, 122.2, 120.9, 105.7, 54.9. Anal. Calcd for $C_{23}H_{16}N_2O\cdot CDCl_3$: C, 63.11; H, 3.97. Found: C, 63.15; H, 4.05.

[2-(8-Methoxy-1-naphthyl)-1,10-phenanthroline][(1,2,3-η)-1,1-dideutero-2-propenyl]palladium Tetrafluoroborate (5). $Pd(dba)_2$ (46.4 mg, 0.081 mmol) and 2-(8-methoxy-1-naphthyl)-1,10-phenanthroline (28.6 mg, 0.085 mmol) were dissolved in methylene chloride (5 mL). 1,1-Dideutero-2-propen-1-ol (10 mg, 0.17 mmol) was added followed by 106 μL of tetrafluoroboric acid solution (0.8 M in 25:1 diethyl ether/methanol, 0.085 mmol). The deep purple color disappeared immediately, and the mixture was stirred at room temperature for 30 min, leaving a dark green solution. After filtration, the solution was concentrated to half its volume, and addition of diethyl ether (8 mL) gave the product as a brownish microcrystalline solid (40 mg, 86% yield). The crude product was dissolved in methylene chloride (2 mL), and diethyl ether was added until substantial amounts of solid formed. After filtration, the filtrate in a small open vial was put in a larger vessel containing diethyl ether and then stored in the freezer overnight. This procedure gave 15 mg of good quality crystals, which were dissolved in CD_2Cl_2 and used in NMR experiments.

(2,9-Dimethyl-1,10-phenanthroline)[(1,2,3-η)-3-methyl-2-butenyl]palladium Chloride (6). $Pd_2(\mu\text{-}Cl)_2$[(1,2,3-η)-3-methyl-2-butenyl]$_2$ (200 mg, 0.47 mmol) and 2,9-dimethyl-1,10-phenanthroline (197 mg, 0.95 mmol) were dissolved in methylene chloride (30 mL). Upon concentration to a small volume the product precipitated as a crystalline solid (370 mg, 92%). Crystallization from methylene chloride and carbon tetrachloride gave yellow crystals suitable for X-ray analysis. These were stored in presence of the mother liquor to avoid loss of crystallization solvent. ^{1}H NMR (400 MHz, $CDCl_3$): δ 8.14 (d, 2 H), 7.90 (s, 2 H), 7.54 (d, 2 H), 5.29 (t, 4 H), 3.80 (br, 1 H), 3.23 (s, 6 H), 3.00 (br, 1 H), 0.66 (s, 3 H), 0.43 (s, 3 H). The ^{1}H NMR spectrum also shows an appreciable amount of the chloride-bridged dimer and free 2,9-dimethyl-1,10-phenanthroline, which presumably is in equilibrium with 6. Anal. Calcd for $C_{19}H_{21}ClN_2Pd\cdot{}^1/_2CH_2Cl_2\cdot{}^1/_2CCl_4$: C, 44.60; H, 4.12; N, 5.20; Cl, 26.33. Found: C, 45.30; H, 4.28; N, 5.40; Cl, 25.68.

Crystal Structure Determination of 6. Many details of the structure analysis carried out on the compound are listed in Table IV. X-ray data were collected at room temperature on an Enraf-Nonius CAD4-F automatic diffractometer, which was operated in the ω/θ scanning mode using Cu Kα graphite-monochromated radiation. The unit cell parameters were obtained by a least-squares fitting of the setting values of 25 strong reflections in the θ range $25° \le \theta \le 29°$. Three monitoring reflections, measured every 500, showed no significant variation of the intensities. In addition to the usual corrections for Lorentz

(20) Baeckström, P.; Stridh, K.; Li, L.; Norin, T. *Acta Chem. Scand.* **1987**, *B41*, 442–447.
(21) Dent, W. D.; Long, R.; Wilkinson, A. J. *J. Chem. Soc.* **1964**, 1585.
(22) Schuetz, R. D.; Millard, F. W. *J. Org. Chem.* **1959**, *24*, 297.
(23) Dehand, J.; Mauro, A.; Ossor, H.; Pfeffer, M.; Santos, R. H. d. A.; Lechat, J. R. *J. Organomet. Chem.* **1983**, *250* (1), 537.
(24) Armarego, W. L. F.; Perrin, D. D. *Purification of Laboratory Chemicals*, 3rd ed.; Pergamon Press: New York, 1988.
(25) The potential complication of scalar relaxation between geminal protons is absent here due to a large shift difference and a very low geminal coupling, usually below 1 Hz.
(26) Dietrich-Buchecker, C. O.; Marnot, P. A.; Sauvage, J. P. *Tetrahedron Lett.* **1982**, *23*, 5291.

Table IV. Summary of Crystallographic Data

cryst size/mm	0.37 × 0.46 × 0.70
formula	$PdClN_2C_{19}H_{21}\cdot{}^1/_2CH_2Cl_2\cdot{}^1/_2CCl_4$
fw	538.6
cryst system	monoclinic
space group	$C2/c$
a/Å	20.190(4)
b/Å	21.278(4)
c/Å	11.501(4)
β	114.76(2)
V/Å^3	4487(2)
Z	8
$F(000)$	2160
D_c/g cm^{-3}	1.59
D_m/g cm^{-3}	1.59
λ(Cu Kα)/Å	1.5418
θ_{max}/deg	74
μ/cm^{-1}	114.0
no. of indep refls	4567
no. of refls above $3\sigma(I)$	2975
no. of refined params	234
goodness of fit	0.942
R	0.054
R_w	0.066

and polarization factors, a semiempirical correction for absorption,[27] which used azimuthal ψ-scan data from two reflections at high χ angle, was applied (maximum and minimum values of the transmission factor were 1.00 and 0.48). The structure was solved by routine application of the Patterson and Fourier techniques. When all non-H atoms of the complex were found, the difference electron density map was carefully scrutinized in order to detect solvent molecules, whose presence was pointed out by the value of the measured density. Maxima around and on a crystallographic 2-fold axis were interpreted as a molecule of CH_2Cl_2, whose carbon atom is in a special position. The crystal packing (Figure 3) shows that the complex molecules form large channels parallel to c, where solvent molecules may be clathrated. Maxima in this region of the Fourier difference map were interpreted as representing one molecule of CCl_4 with an occupancy factor of 0.5. In fact, of the two solvent molecules related by a crystallographic inversion center only one can find enough room to accommodate itself.

As expected from the crystal packing inspection, the molecules of CCl_4 are affected by a much larger positional disorder than CH_2Cl_2, and their refined isotropic thermal parameters converged at high values. The result of the crystallographic analysis of the solvent contained in the unit cell is well consistent with the values of the measured density and of the elemental analysis. It is also in accordance with the ability of the crystals to exchange half of the solvent. The refinement of the structure with isotropic thermal parameters, including solvent molecules and H atoms, converged to $R = 0.087$ and $R_w = 0.110$. The H atoms were added at calculated positions with isotropic thermal parameters 1.2 times higher than the B of the carrier atoms and held fixed during the refinement. At this stage, in order to get a more effective correction of the high absorption effects present in the data, the empirical correction suggested by Walker and Stuart[28] was applied, by using the computer program DIFABS (maximum and minimum values of the absorption correction were 2.35 and 0.81). After this correction the values of the discrepancy indices of isotropic refinement dropped to $R = 0.065$ and $R_w = 0.079$. The final refinement with anisotropic thermal parameters for all non-H atoms except those of the CCl_4 molecules converged to the values presented in Table II. The full-matrix least-squares refinement minimized the quantity $\sum W(\Delta F)^2$ with $W^{-1} = [\sigma^2(F_o) + (0.02F_o)^2 + 2]$, where σ is derived from counting statistics. The final Fourier difference map was within 1.3 e Å^{-3}. Neutral-atomic scattering factors were taken from the literature.[29] All calculations, carried out on a Vax 750 at the Centro Interdipartimentale di Metodologie Chimico-fisiche of the University of Naples, were performed with the Enraf-Nonius (SDP) set of programs.[30]

Lists of bond distances and angles, hydrogen atom parameters, and anisotropic thermal parameters of the non-hydrogen atoms have been deposited as supplementary material.

Acknowledgment. We thank the Swedish board for Technical Development, the Swedish Natural Science Research Council, and the National Research Council of Italy (CNR) for financial support. We thank the Centro Interdipartimentale di Metodologie Chimico-fisiche of the University of Naples for the use of X-ray and computer facilities.

Supplementary Material Available: Tables of positional and thermal parameters of the H atoms (Table Vs), anisotropic thermal parameters of the non-hydrogen atoms (Table VIs), and complete bond distances and angles (Table VIIs) (3 pages). Ordering information is given on any current masthead page.

OM930408N

(27) *International Tables for X-ray Crystallography*; The Kynoch Press: Birmingham, U.K., 1984; Vol. IV.

(28) Walker, N.; Stuart, D. *Acta Crystallogr.* **1983**, *A39*, 158.

(29) North, A. C. T.; Phillips, D. C.; Mathews, F. S. *Acta Crystallogr.* **1968**, *A24*, 351.

(30) B. A. Frenz & Associates Inc. Structure Determination Package (SDP), College Station, TX, and Enraf-Nonius, Delft, The Netherlands, 1982.